Two copies of spin helices with stretching pitch and compensating helicity

Ning Zhao,[1] Yihang Duan,[2] Hao Yang,[1] Xue Li,[1] Wen Liu,[3] Jianhua Zhao,[3] Shixuan Han,[1] Ka Shen,[2] Ning Hao,[4] Jiyong Fu,[1,5,*] and Ping Zhang[1,6,†]

[1]*Department of Physics, Qufu Normal University, Qufu 273165, Shandong, China*
[2]*The Center for Advanced Quantum Studies and Department of Physics, Beijing Normal University, Beijing 100875, China*
[3]*Department of Physics, Jining University, Qufu 273155, Shandong, China*
[4]*Anhui Province Key Laboratory of Condensed Matter Physics at Extreme Conditions, High Magnetic Field Laboratory, HFIPS, Chinese Academy of Sciences, Hefei 230031, China*
[5]*Instituto de Física, Universidade de Brasília, Brasília-DF 70919-970, Brazil*
[6]*Beijing Computational Science Research Center, Beijing 100084, China*

(Received 5 December 2022; revised 14 April 2023; accepted 3 May 2023; published 16 May 2023)

Persistent spin helix (PSH) manifests itself as an effective knob to tackle spin decay inevitably occurring in disordered two-dimensional electron gases. Here, for ordinary (110)-oriented two-subband GaInAs wells subjected to top and back gate voltages, we theoretically achieve adjusting the Dresselhaus terms of the two bands while meanwhile consistently *pinning* the system at symmetric configuration [i.e., locking the Rashba spin-orbit (SO) terms to zero], thus enabling *simultaneous* formation of two copies of PSHs of flexible control. Strikingly, we are able to stretch the pitch—spin density wave length—of PSH by far more than one period, enabling *helix-stretch functional* spin field-effect transistor (FET), with both on and off states protected by the PSH symmetry. Moreover, we attain a scenario in which the helicities of the two copies of PSHs are sufficiently compensated. This makes possible a new concept: "orbit (band) filter," which resembles spin FET while with novel functionality of orbit filtering, opening up a new route towards spintronic and orbitronic combined applications.

DOI: 10.1103/PhysRevB.107.205407

I. INTRODUCTION

The spin-orbit (SO) interaction facilitates coherent spin manipulation [1,2], and is of profound importance for diverse fields of condensed matter such as topological insulators [3] and Majorana fermions [4,5]. However, the SO interaction inevitably causes spin decay and rotation-angle randomization [6–8], which acts as fundamental challenges, not only limiting the functionality of SO based devices such as spin field-effect transistor (FET) but also setting great restrictions in quantum information science.

The persistent spin helix (PSH), which features invariance with respect to spin rotations [SU(2) symmetry] and is robust against any time-reversal conserving interaction [9–17], provides a route to overcome spin decay occurring in disordered two-dimensional electron gases (2DEGs) [18–22]. Since the experimental verification of PSH through transient spin grating spectroscopy [11] and time-resolved Kerr rotation [12], it has been exploited in various different forms including the drifting PSH driven by an in-plane electric field [23–27] and the spin relaxation anisotropy mediated by an external magnetic field [28,29], as well as its recent extension to Josephson junctions [30,31] and even cavity photons [32]. Our recent proposals on the stretchable PSH [33] and its symmetry breaking [34] as well as the PSH-based persistent skyrmion lattice [35], further manifest the importance of PSH.

Here, we theoretically demonstrate the emergence of two copies of PSHs, having not only *stretchy* pitch—spin density wave length—but also *compensating* helicity, in (110)-oriented GaInAs wells with two subbands. We utilize a technique, which relies on a combination of top (V_T) and back (V_B) gates [Fig. 1(a)]. With the help of self-consistent calculation of the Poisson and Schrödinger equations under the Hartree approximation, we obtain a full dual-gate multiband SO control [36]. In particular, we achieve adjusting the Dresselhaus SO couplings of the two bands while meanwhile *locking* the Rashba SO terms to zero, enabling *simultaneous* formation of two copies of PSHs (one for each band). Strikingly, we are able to stretch the pitch of PSH by far more than one period, enabling *helix-stretch functional* spin FET [Fig. 2(a)], which works in two-dimensional (2D) diffusive regime with both on and off states protected by the PSH symmetry. Further, we attain a scenario that the helicities of the two copies of PSHs are sufficiently compensated [Fig. 1(e)], resulting in persistent spin textures in both real and momentum spaces. This makes possible a new concept: "orbit (band) filter" [Fig. 2(b)], which resembles spin FET while with novel functionality of *orbit filtering*, opening up a new route towards spintronic and orbitronic combined applications.

II. THEORETICAL FRAMEWORK: FROM A 3D TO AN EFFECTIVE 2D HAMILTONIAN

We start with the three-dimensional (3D) Rashba-Dresselhaus SO Hamiltonian for electrons hosted in

*yongjf@qfnu.edu.cn
†zhang_ping@iapcm.ac.cn

 ©2023 American Physical Society

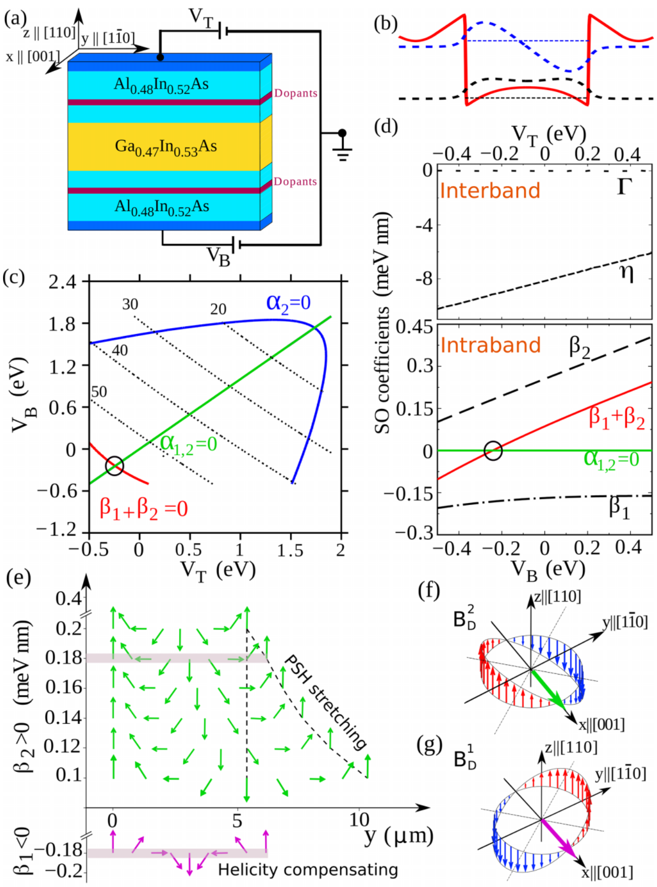

FIG. 1. (a) Growth profile of a (110)-oriented $Al_{0.48}In_{0.52}As/Ga_{0.47}In_{0.53}As$ well subjected to top (V_T) and back (V_B) gates, and (b) its potential profile and wave functions of two subbands. (c) Three distinct regimes of dual-gate SO control: (i) $\alpha_{1,2} = 0$ (green); (ii) $\alpha_2 = 0$ (blue); and (iii) $\beta_1 + \beta_2 = 0$ (red). The contours of constant density (in unit of 10^{11} cm^{-2}; gray) are also shown. (d) SO coefficients (upper panel: interband; lower panel: intraband) against V_T and V_B along the line of $\alpha_{1,2} = 0$ in (c). Black circle in (c) and (d) marks the "overlap" between regimes (i) and (iii). (e) Gate control of two-band PSHs *via* β_ν ($\nu = 1, 2$), the value of which complies with the lower panel in (d). The PSH for band 2 (green arrows) is greatly stretched, though only one period of stretching with β_2 ranging from 0.1 to 0.2 meV · nm is shown, as guided by the vertical and curved (dashed) black lines; the PSH for band 1 (pink arrows) essentially maintains the same pitch, cf. β_1 and β_2 in the lower panel of (d). The shadowed regions at $\beta_1 = -\beta_2 = -0.18$ meV · nm indicate that the helicities of the copies of PSHs are sufficiently compensated. (f), (g) Schematic of opposite Dresselhaus fields for the first (g) and second (f) bands, with $\beta_1 < 0$ and $\beta_2 > 0$.

(110)-oriented wells in a reference frame of $x||[001]$, $y||[1\bar{1}0]$, and $z||[110]$ (for convenience):

$$H = H_{\rm QW} + \beta(z)\sigma_z k_y + \alpha(z)(\sigma_y k_x - \sigma_x k_y), \tag{1}$$

where $H_{\rm QW} = (k_x^2 + k_y^2)/2m^* + k_z^2/2m^* + V_{\rm sc}(z)$ is spin independent, with m^* the effective electron mass, $k_{x,y,z}$ the wave vector components, and $V_{\rm sc}$ the *self-consistent* potential comprising the structural $V_{\rm w}$, the electron Hartree $V_{\rm e}$, the doping $V_{\rm d}$, and the gate $V_{\rm g}(V_{\rm T}, V_{\rm B})$ contributions. The second (third) term describes the Dresselhaus (Rashba) SO interaction, in which $\beta(z) = -(1/2)[k_z\gamma(z)k_z + \gamma(z)(2k_x^2 - k_y^2)]$ and $\alpha(z) = \eta_w \partial_z V_{\rm w} + \eta_H \partial_z (V_{\rm g} + V_{\rm e} + V_{\rm d})$ define the corresponding SO strength [37] and $\sigma_{x,y,z}$ are the spin Pauli matrices. Here, η_w and η_H contain bulk quantities of the well layer [33,35,38], and $\gamma(z)$ the layer-dependent bulk Dresselhaus parameter. Note that, for $\beta(z)$, only dominant terms are kept, as widely done in literatures [8,21,39], and for the other terms, see the Supplemental Material (SM, Sec. I) [40].

By projecting the 3D form [Eq. (1)] onto the two spin-degenerate eigensolutions of $H_{\rm QW}$: $\langle \mathbf{r}|\mathbf{k}, \nu, \sigma\rangle = e^{i\mathbf{k}\cdot\mathbf{r}}\psi_\nu(z)|\sigma_z\rangle$, $\nu = 1, 2$, $\sigma_z = \uparrow, \downarrow$, with energies $\varepsilon_{\nu,k} = \varepsilon_\nu + \hbar^2k^2/2m^*$, where $\mathbf{k}$ is the in-plane electron wave vector and ε_ν is the νth energy level, we obtain the 4×4 2D Hamiltonian

$$\mathcal{H} = \left(\frac{\hbar^2k^2}{2m^*} + \varepsilon_+\right)\mathbb{1}\otimes\mathbb{1} - \varepsilon_-\tau_z\otimes\mathbb{1} + \mathcal{H}_{\rm RD}, \tag{2}$$

in which $\varepsilon_\pm = (\varepsilon_2 \pm \varepsilon_1)/2$, $\tau_{x,y,z}$ denote the "pseudospin" Pauli matrices in the orbital (band) subspace, and $\mathcal{H}_{\rm RD}$ describes the 2D Rashba and Dresselhaus couplings

$$\mathcal{H}_{\rm RD} = \frac{1}{2}g\mu_B \sum_{\nu=1,2}\left[\tau_\nu \otimes \boldsymbol{\sigma}\cdot\mathbf{B}_{\rm SO}^{\nu} + \tau_{\rm x}\otimes\boldsymbol{\sigma}\cdot\mathbf{B}_{\rm SO}^{12}\right], \tag{3}$$

with g the electron g factor, μ_B the Bohr magneton, and $\tau_{1,2} = (\mathbf{1} \pm \tau_z)/2$. The intraband SO field reads

$$\mathbf{B}_{\rm SO}^{\nu} = -\frac{2}{g\mu_{\rm B}}{\rm k}\left[\alpha_\nu(\sin\theta\hat{\mathbf{x}} - \cos\theta\hat{\mathbf{y}}) + \frac{1}{2}\beta_\nu\sin\theta\hat{\mathbf{z}}\right]. \tag{4}$$

Here we have defined $\tan\theta = k_y/k_x$, and the *intraband* SO couplings $\alpha_\nu = \langle\nu|\alpha(z)|\nu\rangle$ (Rashba) and $\beta_\nu = \beta_{1,\nu} - \beta_{3,\nu}$ (Dresselhaus), with $\beta_{1,\nu} = \langle\nu|k_z\gamma(z)k_z|\nu\rangle$ the linear term having interface contribution [2,37] and $\beta_{3,\nu} = \langle\nu|\gamma(z)|\nu\rangle k^2/4$ the cubic renormalization. The interband SO field is written as

$$\mathbf{B}_{\rm SO}^{12} = -\frac{2}{g\mu_{\rm B}}{\rm k}\left[\eta(\sin\theta\hat{\mathbf{x}} - \cos\theta\hat{\mathbf{y}}) + \frac{1}{2}\Gamma\sin\theta\hat{\mathbf{z}}\right], \tag{5}$$

where $\eta = \langle\nu|\alpha(z)|\nu'\rangle$ (Rashba) and $\Gamma = \langle\nu|\beta(z)|\nu'\rangle$ (Dresselhaus) denote the *interband* SO couplings. For detailed derivations of 2D Hamiltonian including both the first and third harmonic terms, see the SM (Sec. I) [40].

III. RESULTS AND DISCUSSION

A. Three distinct regimes for dual-gate SO control

We consider an $Al_{0.48}In_{0.52}As/Ga_{0.47}In_{0.53}As/Al_{0.48}In_{0.52}$ As quantum well grown along the $z||[110]$ direction, of width 24 nm subjected to top (V_T) and back (V_B) gates [Fig. 1(a)], similar to experimental samples of Ref. [41] while with two bands [Fig. 1(b)]. Our structure contains two *symmetrically* doped layers of width 6 nm sitting 18 nm away from either side of the well, with the donor concentration $\rho = 10\times10^{18}$ cm^{-3}. By adjusting V_T and V_B, which may compensate each other in varying the well symmetry, we achieve three distinct regimes for SO control: (i) Rashba terms α_1 and α_2 are simultaneously *locked* to zero, following the well being *pinned* at symmetric configuration [green line in Fig. 1(c)]; (ii) α_2 maintains zero but α_1 is largely finite [blue line in Fig. 1(c)]; and (iii) Dresselhaus terms β_1 and β_2 have equal

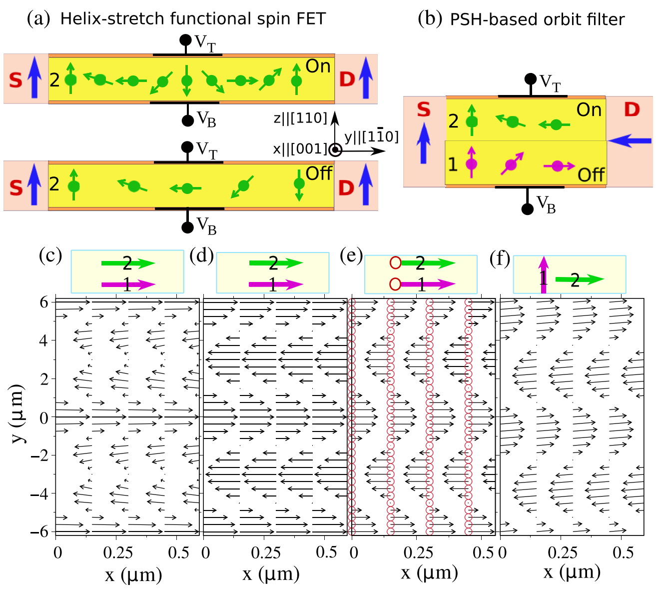

FIG. 2. Side view of dual-gate helix-stretch functional spin FET (a) and orbit filter (b). The labels S and D respectively denote ferromagnetic source and drain with the 2DEG channel sandwiched in between, and 1 (2) stands for the first (second) band. (c)–(f) Coherent superposition of two copies of PSHs, when $\mathbf{s_1}(0) = \mathbf{s_2}(0) = |\uparrow_x\rangle$ (c), (d); $\mathbf{s_1}(0) = \mathbf{s_2}(0) = |\uparrow_{xz}\rangle$ (e); and $\mathbf{s_1}(0) = |\uparrow_y\rangle$, $\mathbf{s_2}(0) = |\uparrow_x\rangle$ (f), where $|\uparrow_{xz}\rangle$ refers to the spin state pointing along the direction bisecting the angle between x and z axes. The size of circles (arrows) denote s_z ($s_{x,y}$), and red circles stand for spin up. In (c), $\beta_2 = -2\beta_1$; in (d)–(f), $\beta_2 = -\beta_1$, with $\beta_1 = -0.18$ meV nm [Fig. 1(e)].

strength but opposite signs [red line in Fig. 1(c)]. These three regimes underlie our PSH control, as we discuss next.

B. PSH pitch stretching and helix-stretch functional spin-FET in symmetric well

In regime (i), since the Rashba α_1 and α_2 both identically vanish, the overall SO field within the νth band is solely determined by the Dresselhaus field $\mathbf{B}_D^\nu$, which is *intrinsically* perpendicular to the 2DEG plane [Figs. 1(f) and 1(g)], ensuring *simultaneous* formation of two copies of PSHs (one for each band). In particular, for band 2, we are able to enhance the Dresselhaus strength β_2 by nearly a factor of four as V_B ($\approx V_T$) varying from -0.5 to 0.5 eV [Fig. 1(d)], resulting in the PSH pitch, $P_2 = 2\pi/Q_2$, $Q_2 = m^*\beta_2/\hbar^2$, a stretch of far more than one period, see the *stretching* green arrows from $y = 5.05$ to 10.05 μm in Fig. 1(e). This offers a unique platform for 2D diffusive spin-FET functioning for disordered electrons [Fig. 2(a)], with both on and off states controlled by $V_g(V_T, V_B)$ and protected by the PSH symmetry, robust against any time-reversal conserving interactions (e.g., disorder). In contrast, regarding band 1, we reveal that β_1 exhibits inertia against $V_g(V_T, V_B)$, thus the corresponding PSH essentially maintains unstretched [pink arrows in Fig. 1(e)].

C. Subband-selective PSH in asymmetric well

The Rashba terms are usually nonzero in structurally asymmetric wells [42]. Interestingly, for 2DEGs of double occupancy, due to delicate interplay of distinct SO contributions from several constituent potentials [i.e., V_w, V_e, V_d, and $V_g(V_T, V_B)$], we reveal that the electrons occupying the second band may see a *local* symmetry such that α_2 vanishes even in the well with an *overall* asymmetry (though α_1 is nonzero). This refers to our regime (ii), in which the PSH only survives for the second band, allowing *subband-selective* PSH control in asymmetric wells. And, here we achieve *continuous* selective control of the PSH, see in Fig. 1(c) the blue line, along which the SO manipulation is given in the SM (Sec. IV) [40].

D. PSHs with compensating helicity: Orbit (pseudospin) filter

We attain a scenario which features an *overlap* between regimes (i) and (iii), namely the relations $\alpha_1 = \alpha_2 = 0$ and $\beta_1 = -\beta_2$ simultaneously hold, see the black circle in Figs. 1(c) and 1(d). The former relation, originating from the well being pinned at symmetric configuration, ensures that the two copies of PSHs—one for each band—form simultaneously. And, the latter one leads to the two PSHs being of not only equal pitch $P_1 = P_2$, $P_\nu = 2\pi/|Q_\nu|$, $Q_\nu = m^*\beta_\nu/\hbar^2$, but also opposite helicity, see in Fig. 1(e) the lower (band 1) and upper (band 2) shadowed regions. The compensating helicity of the two PSHs directly follows from that the first- and second-band electrons see the SO field of opposite directions [cf. Figs. 1(f) and 1(g)].

These features underneath the two copies of PSHs make possible a new concept: "orbit (band) filter." It *resembles* spin FET while embraces novel functionality of *orbit filtering* [Fig. 2(b)], which is controllable by $V_g(V_T, V_B)$, opening up a new route towards spin-orbitronic applications. And, the electrons occupying the first band in Fig. 2(b) are filtered out due to opposite spins between the 2DEG channel and the drain, facilitating band-selective spin manipulation.

In contrast to (110) wells considered here, note that in (001) wells, as we recently proposed persistent skyrmion lattice formed by the so-called two-band "crossed" PSHs [35], the SO fields of the two bands align in the 2DEG plane and are orthogonal. Also, to stretch the PSH in (001) wells, one needs to tune the Rashba and Dresselhaus SO terms *independently* so that the two terms are not only adjusted *simultaneously* but also locked to equal strengths [33,34]. Thus, in practice, it is essentially not feasible to achieve the orbit filter by resorting to a well grown along the (001) direction.

E. Robust persistent spin textures in real space: Spatial superposition of two copies of PSHs

The unidirectional Dresselhaus field for (110) wells defines the persistent spin texture in momentum space [44–47]. Now, we move to spatial superposition of PSHs with compensating helicity. For realistic considerations, we take into account the presence of spin-independent potential $V(\mathbf{r})$, which may arise from a nonmagnetic disorder, to determine *robust* eigenspinors for 2DEGs hosted in (110) wells with two bands. Then, the electron Hamiltonian reads, $\mathcal{H}_{\rm im} = \mathcal{H} + (\mathbb{1} \otimes \mathbb{1})V(\mathbf{r})$, with $\mathcal{H}$ given in Eq. (2). For GaAs and GaInAs based wells of typical electron densities such that the Fermi wave vector is far away from the crossings of energy dispersions of the two bands, the interband terms can be treated as a perturbation [35,48]. Accordingly, we have $\mathcal{H}_{\rm im} \to \sum_\nu \tau_\nu \otimes \mathcal{H}^\nu_{\rm im}$, with $\mathcal{H}^\nu_{\rm im} = [\varepsilon_\nu + \hbar^2 k^2/2m + V(\mathbf{r})]\mathbb{1} + (1/2)g\mu_B B^\nu_{\rm D}\sigma_z$, which admits eigenstates of the form $\psi^{\uparrow_z}_\nu(\mathbf{r}) = \phi(\mathbf{r})e^{i\frac{Q_\nu y}{2}}|\uparrow_z\rangle$ and $\psi^{\downarrow_z}_\nu(\mathbf{r}) = \phi(\mathbf{r})e^{-i\frac{Q_\nu y}{2}}|\downarrow_z\rangle$. Also, the function $\phi(\mathbf{r})$ fulfills the spin-independent equation $[-(\hbar^2/2m^*)\nabla^2 + V(\mathbf{r})]\phi(\mathbf{r}) = (\varepsilon - \varepsilon_\nu + m^*\beta_\nu^2/8\hbar^2)\phi(\mathbf{r})$, where ε is the eigenvalue for either $\psi^{\uparrow_z}_\nu(\mathbf{r})$ or $\psi^{\downarrow_z}_\nu(\mathbf{r})$. Thus, the two spin states are doubly degenerate owing to time reversal symmetry and are robust against any nonmagnetic scatterings. The underlying physics is rooted in the commutation relation $[\mathcal{H}^\nu_{\rm im}, \sigma_z] = 0$, valid for both bands. Next, we construct superposition of two copies of PSHs of compensating helicity.

Let $\psi_\nu(\mathbf{r}) = \phi(\mathbf{r})[\exp(iQ_\nu y/2)|\uparrow_z\rangle + \exp(-iQ_\nu y/2)|\downarrow_z\rangle)]/\sqrt{2}$ such that the stationary spin states at $\mathbf{r} = \mathbf{0}$ point along the x direction for both bands $\nu = 1, 2$. This results in the νth band spin density $\mathbf{s}_\nu(\mathbf{r}) = (1/2)\psi^\dagger_\nu(\mathbf{r})\boldsymbol{\sigma}\psi_\nu(\mathbf{r})$. Then, for coherent superposition of stationary states $\psi(\mathbf{r}) = (1/\sqrt{2})[\psi_1(\mathbf{r}) \oplus \psi_2(\mathbf{r})]$, the overall spin density $\mathbf{s}(\mathbf{r}) = (1/2)\psi^\dagger(\mathbf{r})(\mathbb{1} \otimes \boldsymbol{\sigma})\psi(\mathbf{r})$ reads

$$\mathbf{s}(\mathbf{r}) = \frac{1}{4}|\phi(\mathbf{r})|^2 \sum_\nu [\cos(Q_\nu y)\hat{x} - \sin(Q_\nu y)\hat{y}]. \tag{6}$$

Here the last term of $\sin(Q_\nu y)$, which depends on the sign of β_ν, dominates the helicity of $\mathbf{s}(\mathbf{r})$. Besides the quantum-mechanical approach, we also obtain Eq. (6) *via* the semiclassical approach based on 2D diffusive kinetic equation [26,27] (see the SM, Sec. V) [40]. Accordingly, in the scenario of $\beta \equiv \beta_1$ $(= -\beta_2)$, i.e., $Q \equiv Q_1$ $(= -Q_2)$, the helicity of the overall spin density vanishes as a result of the helicities of $\mathbf{s}_1$ and $\mathbf{s}_2$ being sufficiently compensated (see the SM, Sec. III) [40], leading to persistent (unidirectional) spin texture even in real space [Fig. 2(d)]. Without lack of generality, to obtain Fig. 2(d), we have taken $|\phi(\mathbf{r})|^2 = 1$, referring to weak disorder, for which $\phi(\mathbf{r}) \to \exp(i\mathbf{k}\cdot\mathbf{r})$. In contrast, when β_1 and β_2 have different magnitudes, the overall spin density $\mathbf{s}(\mathbf{r})$ still displays partial helicity, owing to distinct pitches of the two-band PSHs [Fig. 2(c)]. In addition, when both $\mathbf{s_1}$ and $\mathbf{s_2}$ at $\mathbf{r} = 0$ are oriented in a direction bisecting the x and z axes, the s_x component exhibits similar spatial distribution to that in Fig. 2(d), while the s_z component maintains unchanged as it aligns with the Dresselhaus field [cf. Figs. 2(e) and 2(d)]. Further, it is noteworthy that in the case of $\beta_1 = -\beta_2$, even when $\mathbf{s_1}(0)$ and $\mathbf{s_2}(0)$ point along distinct directions [49], e.g., y and x directions for bands 1 and 2, respectively, the helicity of coherently superimposed $\mathbf{s}(\mathbf{r})$ also vanishes [Fig. 2(f)].

F. The interband SO (Γ and η) contributions: Band dispersion, spin texture, and spin relaxation

For the well being pinned at symmetric configurations so that the two copies of PSHs form simultaneously, we reveal that the interband Dresselhaus Γ vanishes due to distinct parities of the wave functions of the two bands [upper panel of Fig. 1(d)], similar to intraband Rashba α_ν. When β_1 and β_2 have opposite signs, referring to the scenario of two PSHs having compensating helicity, we observe that η maintains the feature of crossing of uncoupled ($\eta = 0$) band dispersions, as indicated by the spin-polarized electronic structure in Fig. 3(a). Clearly, the spins for all the four energy branches (two for each band) remain invariant, which indicates that the spin states maintain unhybridized even in the presence of interband coupling, greatly quenching the detrimental effect of η on the two copies of PSHs. Also, the D'yakonov-Perel spin relaxation [50] due to either third harmonic terms or interband corrections is suppressed, as both factors do not alter the fundamental symmetry of the SO field in (110)-oriented wells (see the SM, Secs. I and II) [40]. While the interband scattering may lead to the Elliott-Yafet type spin relaxation [8,51,52] we obtain, the relaxation time is comparable to that of the cubic Dresselhaus (D'yakonov-Perel type) in (001) wells [10–12] in limiting the PSH lifetime (see the SM, Sec. VI) [40]. All these justify our proposed two copies of PSHs as well as the related applications (e.g., diffusive spin-FET and orbit filter) in (110) wells being feasible for experimental realizations.

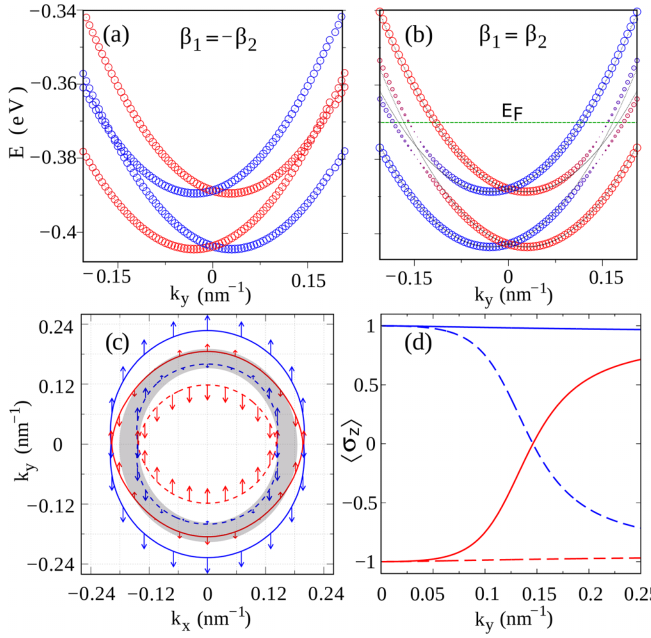

FIG. 3. (a) Spin-resolved energy dispersion (scaled by a factor of 50 for visibility) for the (110) well in the scenario of $\beta_1 = -\beta_2$, $\alpha_{1,2} = 0$ (intraband), and $\Gamma = 0$, $\eta \neq 0$ (interband), as marked by black circle in Figs. 1(c) and 1(d). The size of circles denotes the magnitude of spin and the color stands for s_z, with the red (blue) referring to spin up (down), indicating that there is no spin hybridization occurring. (b) A counterpart to (a) while with β_1 and β_2 having the same sign. (c) Constant energy contours and spin textures at $E = E_{\rm F} = -0.37$ eV [see (b)] [43]. The shadowed region indicates spin hybridization of distinct spin branches. (d) $\langle\sigma_z\rangle$ versus k_y, with the line type (and color) corresponding to respective energy branches in (c). The parameters in (c) and (d) are the same as those in (b).

For a full picture, in Fig. 3(b) we show the spin-resolved electronic structure for the *usual* scenario of β_1 and β_2 having the same sign [e.g., see the SM, Fig. S2] [40]. Clearly, the original crossing for the uncoupled bands turns to be an avoided crossing, cf. black lines and colored circles. By setting the Fermi level $E_{\rm F} = -0.37$ eV [43], we also reveal anisotropic energy dispersions and the spin hybridization between the middle two branches, see the shadowed region in Fig. 3(c). And, the spin polarization may even vanish near the avoided crossing [Fig. 3(d)]. These vertex corrections due to interband effect may lead to intriguing possibilities for spintronic applications, e.g., high-efficiency spin-charge conversion devices [53].

IV. CONCLUDING REMARKS

Multiband SO phenomena are now attracting growing interest [35,54–57]. Here, focusing on (110) GaInAs wells with two bands, we have achieved three distinct regimes of dual-gate SO manipulation, and further demonstrated the emergence of two copies of PSHs with not only stretchy pitch but also compensating helicity. Benefiting from them, we have not only proposed helix-stretch functional spin FET with both on and off states protected by the PSH symmetry, but also put forward a new concept: "orbit (band) filter," opening up a new avenue for spintronic and orbitronic combined applications. Our work would attract diverse interests in the communities of spintronics, orbitronics, and even quantum information science requiring long time and long-ranged coherent spin control. As a final remark, similar SO control can also be achieved *via* optical means that we recently proposed in Ref. [58], by resorting to intense high-frequency laser fields (see also the SM, Sec. VII) [40], making our results more reliable for experimental realizations.

ACKNOWLEDGMENTS

We thank Yang Zhou and Denis R. Candido for valuable discussions about spin relaxation and quantum computing, respectively. This work was supported by the National Natural Science Foundation of China (Grants No. 12274256, No. 11874236, No. 11974047, No. 12022413, No. 92265104, and No. 11674331), the Major Basic Program of Natural Science Foundation of Shandong Province (Grant No. ZR2021ZD01), the National Key R&D Program of China (Grant No. 2022YFA1403200), and the "Strategic Priority Research Program (B)" of the Chinese Academy of Sciences (Grant No. XDB33030100). S.X.H. was partially supported by Shandong Provincial Natural Science Foundation (Grant No. ZR2019BA007). W.L. acknowledges financial support from the Higher Educational Youth Innovation Science and Technology Program of Shandong Province (Grant No. 2019KJJ010).

[1] D. Awschalom, D. Loss, and N. Samarth, *Semiconductor Spintronics and Quantum Computation* (Springer, New York, 2002).
[2] I. Žutić, J. Fabian, and S. D. Sarma, Spintronics: Fundamentals and applications, Rev. Mod. Phys. **76**, 323 (2004).
[3] B. A. Bernevig, T. L. Hughes, and S. C. Zhang, Quantum spin Hall effect and topological phase transition in HgTe quantum wells, Science **314**, 1757 (2006).
[4] R. M. Lutchyn, J. D. Sau, and S. Das Sarma, Majorana Fermions and a Topological Phase Transition in Semiconductor-Superconductor Heterostructures, Phys. Rev. Lett. **105**, 077001 (2010).
[5] Y. Oreg, G. Refael, and F. von Oppen, Helical Liquids and Majorana Bound States in Quantum Wires, Phys. Rev. Lett. **105**, 177002 (2010).
[6] M. I. Dyakonov and V. Y. Kachorovskii, Spin relaxation of two-dimensional electrons in non-centrosymmetric semiconductors, Sov. Phys. Semicond. **20**, 110 (1986).
[7] Y. Yafet, Conduction electron spin relaxation in the superconducting state, Phys. Lett. A **98**, 287 (1983).
[8] S. Döhrmann, D. Hägele, J. Rudolph, M. Bichler, D. Schuh, and M. Oestreich, Anomalous Spin Dephasing in (110) GaAs Quantum Wells: Anisotropy and Intersubband Effects, Phys. Rev. Lett. **93**, 147405 (2004).
[9] J. Schliemann, J. C. Egues, and D. Loss, Nonballistic Spin-Field-Effect Transistor, Phys. Rev. Lett. **90**, 146801 (2003).
[10] B. A. Bernevig, J. Orenstein, and S. C. Zhang, Exact SU(2) Symmetry and Persistent Spin Helix in a Spin-Orbit Coupled System, Phys. Rev. Lett. **97**, 236601 (2006).
[11] J. D. Koralek, C. P. Weber, J. Orenstein, B. A. Bernevig, S. C. Zhang, S. Mack, and D. D. Awschalom, Emergence of the persistent spin helix in semiconductor quantum wells, Nature (London) **458**, 610 (2009).
[12] M. P. Walser, C. Reichl, W. Wegscheider, and G. Salis, Direct mapping of the formation of a persistent spin helix, Nat. Phys. **8**, 757 (2012).
[13] PSH patterns for 2DEGs in the ballistic regime were studied by M. H. Liu, K. W. Chen, S. Chen, and C. Chang, Phys. Rev. B **74**, 235322 (2006). In addition, PSHs in hole gases can be found in T. Dollinger, M. Kammermeier, A. Scholz, P. Wenk, J. Schliemann, K. Richter, and R. Winkler, **90**, 115306 (2014).
[14] J. Schliemann, Colloquium: Persistent spin textures in semiconductor nanostructures, Rev. Mod. Phys. **89**, 011001 (2017).
[15] M. Kohda and G. Salis, Physics and application of persistent spin helix state in semiconductor heterostructures, Semicond. Sci. Technol. **32**, 073002 (2017).
[16] S. Anghel, A. V. Poshakinskiy, K. Schiller, G. Yusa, T. Mano, T. Noda, and M. Betz, Spin helices in GaAs quantum wells: Interplay of electron density, spin diffusion, and spin lifetime, J. Appl. Phys. **132**, 054301 (2022).
[17] L. Y. Yang, J. D. Koralek, J. Orenstein, D. R. Tibbetts, J. L. Reno, and M. P. Lilly, Coherent Propagation of Spin Helices in a Quantum-Well Confined Electron Gas, Phys. Rev. Lett. **109**, 246603 (2012).
[18] J. Fabian, Spin's lifetime extended, Nature (London) **458**, 580 (2009).
[19] Y. Kunihashi, M. Kohda, H. Sanada, H. Gotoh, T. Sogawa, and J. Nitta, Proposal of spin complementary field effect transistor, Appl. Phys. Lett. **100**, 113502 (2012).
[20] D. Iizasa, M. Kohda, U. Zülicke, J. Nitta, and M. Kammermeier, Enhanced longevity of the spin helix in low-symmetry quantum wells, Phys. Rev. B **101**, 245417 (2020).
[21] D. Iizasa, D. Sato, K. Morita, J. Nitta, and M. Kohda, Robustness of a persistent spin helix against a cubic Dresselhaus field

in (001) and (110) oriented two-dimensional electron gases, Phys. Rev. B **98**, 165112 (2018).
[22] Y. S. Chen, S. Fält, W. Wegscheider, and G. Salis, Unidirectional spin-orbit interaction and spin-helix state in a (110)-oriented GaAs/(Al,Ga)As quantum well, Phys. Rev. B **90**, 121304(R) (2014).
[23] P. Altmann, F. G. G. Hernandez, G. J. Ferreira, M. Kohda, C. Reichl, W. Wegscheider, and G. Salis, Current Controlled Spin Precession of Quasistationary Electrons in a Cubic Spin-Orbit Field, Phys. Rev. Lett. **116**, 196802 (2016).
[24] Y. Kunihashi, H. Sanada, H. Gotoh, K. Onomitsu, M. Kohda, J. Nitta, and T. Sogawa, Drift transport of helical spin coherence with tailored spin-orbit interactions, Nat. Commun. **7**, 10722 (2016).
[25] S. Anghel, A. V. Poshakinskiy, K. Schiller, F. Passmann, C. Ruppert, S. A. Tarasenko, G. Yusa, T. Mano, T. Noda, and M. Betz, Anisotropic expansion of drifting spin helices in GaAs quantum wells, Phys. Rev. B **103**, 035429 (2021).
[26] K. Shen, R. Raimondi, and G. Vignale, Theory of coupled spin-charge transport due to spin-orbit interaction in inhomogeneous two-dimensional electron liquids, Phys. Rev. B **90**, 245302 (2014).
[27] K. Shen and G. Vignale, Collective Spin Hall Effect for Electron-Hole Gratings, Phys. Rev. Lett. **111**, 136602 (2013).
[28] D. Iizasa, A. Aoki, T. Saito, J. Nitta, G. Salis, and M. Kohda, Control of spin relaxation anisotropy by spin-orbit-coupled diffusive spin motion, Phys. Rev. B **103**, 024427 (2021).
[29] J. Ishihara, Y. Ohno, and H. Ohno, Direct imaging of gate-controlled persistent spin helix state in a modulation-doped GaAs/AlGaAs quantum well, Appl. Phys. Express **7**, 013001 (2014).
[30] M. Alidoust, Critical supercurrent and φ_0 state for probing a persistent spin helix, Phys. Rev. B **101**, 155123 (2020).
[31] M. Alidoust, C. H. Shen, and I. Žutić, Cubic spin-orbit coupling and anomalous josephson effect in planar junctions, Phys. Rev. B **103**, L060503 (2021).
[32] M. Krol, K. Rechcinska, H. Sigurdsson, P. Oliwa, R. Mazur, P. Morawiak, W. Piecek, P. Kula, P. G. Lagoudakis, M. Matuszewski, W. Bardyszewski, B. Pietka, and J. Szczytko, Realizing Optical Persistent Spin Helix and Stern-Gerlach Deflection in an Anisotropic Liquid Crystal Microcavity, Phys. Rev. Lett. **127**, 190401 (2021).
[33] F. Dettwiler, J. Y. Fu, S. Mack, P. J. Weigele, J. C. Egues, D. D. Awschalom, and D. M. Zumbühl, Stretchable Persistent Spin Helices in GaAs Quantum Wells, Phys. Rev. X **7**, 031010 (2017).
[34] P. J. Weigele, D. C. Marinescu, F. Dettwiler, J. Y. Fu, S. Mack, J. C. Egues, D. D. Awschalom, and D. M. Zumbühl, Symmetry breaking of the persistent spin helix in quantum transport, Phys. Rev. B **101**, 035414 (2020).
[35] J. Y. Fu, P. H. Penteado, M. O. Hachiya, D. Loss, and J. C. Egues, Persistent Skyrmion Lattice of Noninteracting Electrons with Spin-Orbit Coupling, Phys. Rev. Lett. **117**, 226401 (2016).
[36] For (001) wells with one subband, we have obtained SO manipulation with great agreement between theory and experiment in Ref. [33].
[37] H. Yang, Q. X. Wang, and J. Y. Fu, Interface involved Dresselhaus spin-orbit coupling in GaInAs/AlInAs heterostructures, Phys. Rev. B **104**, 125426 (2021).
[38] J. Y. Fu and J. C. Egues, Spin-orbit interaction in GaAs wells: From one to two subbands, Phys. Rev. B **91**, 075408 (2015).
[39] T. Hassenkam, S. Pedersen, K. Baklanov, A. Kristensen, C. B. Sorensen, P. E. Lindelof, F. G. Pikus, and G. E. Pikus, Spin splitting and weak localization in (110) GaAs/$Al_xGa_{1-x}As$ quantum wells, Phys. Rev. B **55**, 9298 (1997).
[40] See Supplemental Material at http://link.aps.org/supplemental/10.1103/PhysRevB.107.205407 for detailed derivation from 3D to 2D Hamiltonians, complete form of spin-orbit fields, semiclassical description of two copies of spin helices with compensating helicity, spin relaxation, and the laser field control of spin-orbit couplings (see also Refs. [59–82] therein).
[41] T. Koga, J. Nitta, T. Akazaki, and H. Takayanagi, Rashba Spin-Orbit Coupling Probed by the Weak Antilocalization Analysis in InAlAs/InGaAs/InAlAs Quantum Wells as a Function of Quantum Well Asymmetry, Phys. Rev. Lett. **89**, 046801 (2002).
[42] Y. A. Bychkov and E. I. Rashba, Properties of a 2D electron gas with lifted spectral degeneracy, JETP Lett. **39**, 78 (1984).
[43] In Figs. 3(a) and 3(b), the Fermi level E_F in our wells is in general far below the crossings of the two-band energy dispersions [48], while here we set E_F at −0.37 eV and enlarged SO parameters intending to capture the intriguing hybridized spin textures near the crossing points.
[44] L. L. Tao and E. Y. Tsymbal, Persistent spin texture enforced by symmetry, Nat. Commun. **9**, 2763 (2018).
[45] J. Y. Ji, F. Lou, R. Yu, J. S. Feng, and H. J. Xiang, Symmetry-protected full-space persistent spin texture in two-dimensional materials, Phys. Rev. B **105**, L041404 (2022).
[46] H. Q. Ai, X. K. Ma, X. F. Shao, W. F. Li, and M. W. Zhao, Reversible out-of-plane spin texture in a two-dimensional ferroelectric material for persistent spin helix, Phys. Rev. Mater. **3**, 054407 (2019).
[47] H. J. Zhao, H. Nakamura, R. Arras, C. Paillard, P. Chen, J. Gosteau, X. Li, Y. Yang, and L. Bellaiche, Purely Cubic Spin Splittings with Persistent Spin Textures, Phys. Rev. Lett. **125**, 216405 (2020).
[48] In the (110) wells under symmetric configurations, the intraband Rashba terms α_ν ($\nu = 1, 2$) vanish, and the crossings of the two subband energy dispersions occur at $k_c = 2(\varepsilon_2 - \varepsilon_1)/(\beta_2 - \beta_1)$. With our self-consistent calculations on SO terms, with $\varepsilon_2 - \varepsilon_1 \sim 10$ meV, and $\beta_1 = -\beta_2 = -0.18$ meV nm [see the black circle in Fig. 1(d)], we obtain $k_c \sim 58\ \mathrm{nm}^{-1}$, far larger than the Fermi wave vector $k_F \sim 0.1\ \mathrm{nm}^{-1}$.
[49] While Cruiz and Luiz proposed that the injected current that is initially unpolarized could be divided into two spin-up and spin-down branches [83], so far it is still challenging to make the spin injection into different bands with distinct spins.
[50] M. D'yakonov, V. Marushchak, V. Perel', and A. Titkov, The effect of strain on the spin relaxation of conduction electrons in III-V semiconductors, Sov. Phys. JETP **63**, 655 (1986).
[51] D. Hägele, S. Döhrmann, Rudolph, and M. J. Oestreich, Electron spin relaxation in semiconductors, Adv. Solid State Phys. **45**, 253 (2005).
[52] Y. Zhou and M. W. Wu, A virtual intersubband spin-flip spin-orbit coupling induced spin relaxation in GaAs (110) quantum wells, Solid State Commun. **149**, 2078 (2009).
[53] R. Song, N. Hao, and P. Zhang, Giant inverse Rashba-Edelstein effect: Application to monolayer $OsBi_2$, Phys. Rev. B **104**, 115433 (2021).

[54] F. G. G. Hernandez, G. J. Ferreira, M. Luengo-Kovac, V. Sih, N. M. Kawahala, G. M. Gusev, and A. K. Bakarov, Electrical control of spin relaxation anisotropy during drift transport in a two-dimensional electron gas, Phys. Rev. B **102**, 125305 (2020).

[55] F. G. G. Hernandez, S. Ullah, G. J. Ferreira, N. M. Kawahala, G. M. Gusev, and A. K. Bakarov, Macroscopic transverse drift of long current-induced spin coherence in two-dimensional electron gases, Phys. Rev. B **94**, 045305 (2016).

[56] G. J. Ferreira, F. G. G. Hernandez, P. Altmann, and G. Salis, Spin drift and diffusion in one- and two-subband helical systems, Phys. Rev. B **95**, 125119 (2017).

[57] I. R. de Assis, R. Raimondi, and G. J. Ferreira, Spin drift-diffusion for two-subband quantum wells, Phys. Rev. B **103**, 165304 (2021).

[58] X. Li, W. Wang, N. Zhao, H. Yang, S. X. Han, W. Liu, H. L. Wang, F. Y. Qu, N. Hao, J. Y. Fu, and P. Zhang, Intense high-frequency laser-field control of spin-orbit coupling in GaInAs/AlInAs quantum wells: A laser dressing effect, Phys. Rev. B **106**, 155420 (2022).

[59] G. Dresselhaus, Spin-orbit coupling effects in zinc blende structures, Phys. Rev. **100**, 580 (1955).

[60] R. S. Calsaverini, E. Bernardes, J. C. Egues, and D. Loss, Intersubband-induced spin-orbit interaction in quantum wells, Phys. Rev. B **78**, 155313 (2008).

[61] J. Fabian, A. Matos-Abiague, C. Ertler, P. Stano, and I. Žutić, Semiconductor Spintronics, Acta Phys. Slovaca **57**, 565 (2007).

[62] G. Bastard, *Wave Mechanics Applied to Semiconductor Heterostructures* (Halsted, Les Ulis, New York, 1989).

[63] L. Dekar, L. Chetouani, and T. F. Hammann, Wave function for smooth potential and mass step, Phys. Rev. A **59**, 107 (1999).

[64] R. Vaxenburg and E. Lifshitz, Alloy and heterostructure architectures as promising tools for controlling electronic properties of semiconductor quantum dots, Phys. Rev. B **85**, 075304 (2012).

[65] A. Sashchiuk, D. Yanover, A. Rubin-Brusilovski, G. I. Maikov, R. K. Capek, R. Vaxenburg, J. Tilchin, G. Zaiats, and E. Lifshitz, Tuning of electronic properties in IV-VI colloidal nanostructures by alloy composition and architecture, Nanoscale **5**, 7724 (2013).

[66] Y. J. Jang, A. Shapiro, M. Isarov, A. Rubin-Brusilovski, A. Safran, A. K. Budniak, F. Horani, J. Dehnel, A. Sashchiuk, and E. Lifshitz, Interface control of electronic and optical properties in IV-VI and II-VI core/shell colloidal quantum dots: A review, Chem. Commun. **53**, 1002 (2017).

[67] X. Q. Hou, Y. Li, H. Y. Qin, and X. G. Peng, Effects of interface-potential smoothness and wavefunction delocalization on Auger recombination in colloidal CdSe-based core/shell quantum dots, J. Chem. Phys. **151**, 234703 (2019).

[68] R. Raimondi and P. Schwab, Interplay of intrinsic and extrinsic mechanisms to the spin Hall effect in a two-dimensional electron gas, Phys. E **42**, 952 (2010).

[69] W. C. Henneberger, Perturbation Method for Atoms in Intense Light Beams, Phys. Rev. Lett. **21**, 838 (1968).

[70] Q. Fanyao, A. L. A. Fonseca, and O. A. C. Nunes, Hydrogenic impurities in a quantum well wire in intense, high-frequency laser fields, Phys. Rev. B **54**, 16405 (1996).

[71] C. K. Choi, W. C. Henneberger, and F. C. Sanders, Intensity-dependent ionization potentials for H and He in intense laser beams, Phys. Rev. A **9**, 1895 (1974).

[72] J. I. Gersten and M. H. Mittleman, The shift of atomic states by laser fields, J. Phys. B **9**, 2561 (1976).

[73] C. A. S. Lima and L. C. M. Miranda, Atoms in superintense laser fields, Phys. Rev. A **23**, 3335 (1981).

[74] C. A. S. Lima and L. C. M. Miranda, Hydrogen atom in superintense laser fields: Correction to the ground-state energy, Phys. Lett. A **86**, 367 (1981).

[75] M. Gavrila and J. Z. Kamiński, Free-Free Transitions in Intense High-Frequency Laser Fields, Phys. Rev. Lett. **52**, 613 (1984).

[76] H. Zimmermann, S. Meise, A. Khujakulov, A. Magaña, A. Saenz, and U. Eichmann, Limit on Excitation and Stabilization of Atoms in Intense Optical Laser Fields, Phys. Rev. Lett. **120**, 123202 (2018).

[77] E. Ozturk, H. Sari, and I. Sokmen, Electric field and intense laser field effects on the intersubband optical absorption in a graded quantum well, J. Phys. D **38**, 935 (2005).

[78] B. McNeil and N. Thompson, X-ray free-electron lasers, Nat. Photon. **4**, 814 (2010).

[79] N. Picqué and T. Hänsch, Frequency comb spectroscopy, Nat. Photon. **13**, 146 (2019).

[80] Z. N. Chaleshtari, A. Haghighatzadeh, and A. Attarzadeh, Investigating the effect of position-dependent effective mass on the valence-band electronic states of GaAs/GaAsSb/GaAs parabolic quantum wells modulated by intense laser fields, Solid State Commun. **353**, 114870 (2022).

[81] F. Y. Qu, A. L. A. Fonseca, and O. A. C. Nunes, Intense laser field effect on confined hydrogenic impurities in quantum semiconductors, physica status solidi (b) **197**, 349 (1996).

[82] A. L. A. Fonseca, M. A. Amato, and O. A. C. Nunes, Intense field effects on impurities in semiconductors, physica status solidi (b) **186**, K57 (1994).

[83] H. Cruz and D. Luis, Possibility of spin device in a triple quantum well system, J. Appl. Phys. **104**, 083715 (2008).